Effect of Mn Substitution for Multiferroic $BiFeO_3$ Probed by High-Resolution Soft-X-Ray Spectroscopy

Tohru HIGUCHI, Takeshi HATTORI, Wataru SAKAMOTO,[1] Naoyuki ITOH,[1] Tetsuo SHIMURA,[1] Toshinobu YOGO,[1] Peng YAO,[2] Yi-Sheng LIU,[2] Per-Anders GLANS,[2] Chinglin CHANG,[3] Ziyu WU[4] and Jinghua GUO[2]

Department of Applied Physics, Tokyo University of Science, Tokyo 162-8601, Japan
[1] *EcoTopia Science Institute, Nagoya University, Nagoya 464-8603, Japan*
[2] *Advanced Light Source, Lawrence Berkeley National Laboratory, CA 94720, USA*
[3] *Department of Physics, Tamkang University, Tamsui 251, Taiwan, ROC*
[4] *Beijing Synchrotron Radiation Facility, Institute of High Energy Physics, Chinese Academy of Sciences, Beijing 100049, China*

(Received:)

The electronic structures of $BiFeO_3$ (BF) and Mn-doped $BiFeO_3$ (BF(Mn)) have been studied by X-ray absorption spectroscopy (XAS) and soft-X-ray emission spectroscopy (SXES). The BF and BF(Mn) have the mixed valence state of Fe^{2+} and Fe^{3+}. The valence band is mainly composed of O 2*p* state hybridized with the majority-spin t_{2g} and e_g orbitals of Fe 3*d* state. The conduction band is composed of the minority-spin t_{2g} and e_g orbitals of Fe 3*d*. The band gaps of BF and BF(Mn) are estimated to be 1.3 eV and 2.7 eV, respectively. The increase of band gap with Mn substitution contributes to the change of bandwidth of valence band.

KEYWORDS: $BiFeO_3$ (BF), Mn-doped $BiFeO_3$(BF(Mn)), Multiferroic, X-ray absorption spectroscopy (XAS), soft-X-ray emission spectroscopy (SXES), electronic structure, valence state, electron correlation

1. Introduction

Multiferoic $BiFeO_3$ (BF) is a suitable candidate for attaining ferroelectric and antiferromagnetic domain couplings at room temperature (RT), owing to its high Curie temperature of 1100 K and its high Neel temperature of ~643 K.[1,2] The crystal structure of BF single crystal is a rhombohedrally distorted perovskite structure, which belongs to the space group *R3C* with the unit cell parameters a=3.96 Å and α=89.4 °.[3] In term of ferroelectricity, the BF single crystal has a spontaneous polarization of 3.5 $\mu C/cm^2$ along the <100> direction and of 6.1 $\mu C/cm^2$ along the <111> direction.[4]

In recent years, a large polarization above ~50 $\mu C/cm^2$ has been observed in high quality single crystal and thin films fabricated by pulsed laser deposition (PLD) and chemical solution deposition (CSD).[5-10] The large polarization is effective for application of novel memory and sensor devices. A major problem of BF thin film is low electrical resistivity, which affects the measurement of dielectric/ferroelectric properties at room temperature. The low electrical resistivity of BF thin films is attributed to the valence fluctuations of Fe ions (Fe^{2+} or Fe^{3+}) due to oxygen vacancies.[11,12] Therefore, the formation of solid solutions with other perovskite materials as well as the substitution of impurity atoms at the Bi and Fe sites have been attempted.[13-15] In particular, Sakamoto *et al.* has reported that the resistivity of BF is

greatly improved by a small amount of Mn substitution. The authors believe that the electrical properties of Mn-doped $BiFeO_3$ (BF(Mn)) are closely related to the electronic structures, such as band gap, hybridization effect and valence state. However, the electronic structures of BF and BF(Mn) have not been clarified experimentally thus far.

In this study, the electronic structures of BF and BF(Mn) bulk crystals have been measured by X-ray absorption spectroscopy (XAS) and soft-X-ray emission spectroscopy (SXES). Although photoemission spectroscopy (PES) has been a powerful method of studying of the electronic structure of total density-of-state (DOS), PES cannot study the electronic structure of insulating material due to charging up. Therefore, it is difficult to study the electronic structure of $BiFeO_3$ by PES. SXES is related directly to the occupied DOS.[16] SXES detects the electronic structure of the bulk state owing to the long mean free path of the soft-X-rays. The partial-DOS (PDOS) localized at an atom can be obtained from SXES spectra, because SXES has a clear selection rule regarding the angular momentum due to dipole selection. XAS is related directly to the unoccupied DOS.[17] This optical process is a local process, because of the localized core state. It is governed by the dipole selection rules so that XAS provides spectra related to the site- and symmetry-selected DOS. In this paper, the authors discuss about the effect of Mn substitution for BF.

2. Experimental

$BiFeO_3$ and Mn-doped $BiFeO_3$ samples were prepared by a solid state reaction involving conventional milling and firing techniques. Bi_2O_3, Fe_2O_3 and Mn_2O_3 powders corresponding to BF and 0.8 mol% Mn-doped BF [BF(Mn)] compositions with 0.75 mol% of excess Bi were weighed and thoroughly mixed using stabilized ZrO_2 balls in ethanol. The mixtures were dried, pressed, and calcined at 750~800°C for 2 h at a rate of 10°C/min. In this case, polyvinyl alcohol was used as a binder. The powder compacts were subsequently sintered at 900~1000°C for 3~10 h at a rate of 10°C/min. The prepared samples were characterized by X-ray diffraction with CuKα radiation using a monochromator, a vibrating sample magnetometer, and a *P-E* hysteresis loop measurement system using a Sawyer-Tower circuit. The dielectric loss (tanδ) decreased by Mn substitution (tanδ<5%). Furthermore, the electrical resistivity also increases by Mn substitution. Details have been reported in ref. 15).

XAS and SXES spectra were measured at beamline 7.0.1 at the Advanced Light Source (ALS), Lawrence Berkeley National Laboratory, U.S.A. This beamline is equipped with a spherical grating monochromator.[18] The XAS spectra were obtained by recording the fluorescence yield with 0.2 eV resolution and normalized to the

photocurrent from a clean gold mesh to correct the intensity fluctuation of the excitation beam, which reflects the bulk state. SXES spectra were recorded using a Nordgren-type grazing-incidence spherical grating spectrometer.[19,20] The incidence angle of the photon beam was 20 ° to the sample surface in order to reduce the self-absorption effect. The $BiFeO_3$ sample was fractured before measurement. The SXES spectra were normalized by measurement time and beam current. The SXES spectrometer was set to have a resolution of 0.5 eV for O 1*s* core level and 0.7 eV for Fe 2*p* core level.

3. Results and Discussion

Figure 1 shows the Fe 2*p* XAS spectra of BF and BF(Mn). The Fe 2*p* XAS spectra correspond to the transition from the Fe 2*p* core level to the unoccupied Fe 3*d* state.[21,22] The spectra are derived from $L_3(2p_{3/2})$ at ~710 eV and $L_2(2p_{1/2})$ at ~725 eV. As reference, the Fe 2*p* XAS spectrum of $LaFeO_3$ is also shown as a dashed line. The main component of the $LaFeO_3$ ground state is high-spin $3d^5$, which becomes a $(t_{2g})^3(e_g)^2$ configuration with a total symmetry given by the term symbol $^6A_{1g}$ in octahedral field.[21] The spectral shape of BF and BF(Mn) are similar to that of $LaFeO_3$. This indicates that BF and BF(Mn) have same electronic configuration of $LaFeO_3$.

However, the peaks of BF and BF(Mn) locate on a lower energy side than that of $LaFeO_3$. These behaviors indicate that the Fe valence states of BF and BF(Mn) are the mixed valence state of Fe^{2+} and Fe^{3+}. From the analysis of peak position, the Fe^{2+} valence state is included ~5.0 % in BF and ~4.5 % in BF(Mn). The remnant Mn electron of 0.3 % is considered to enter into Fe^{3+} site.

Figure 2 shows Mn 2*p* XAS spectrum of BF(Mn). The Mn 2*p* XAS spectra correspond to the transition from the Mn 2*p* core level to the unoccupied Mn 3*d* state. Because the Mn concentration is few, the spectrum has a background and their intensities are very low. The spectrum is derived from $L_3(2p_{3/2})$ at ~642 eV and $L_2(2p_{1/2})$ at ~653 eV. As reference, the Mn 2*p* XAS spectrum of $LaMnO_3$ is also shown as a dashed line. The main component of the $LaMnO_3$ ground state is $3d^4$, which becomes a $(t_{2g})^3(e_g)^1$ configuration in an octahedral field. The peak position of BF(Mn) accords with that of $LaMnO_3$. Furthermore, the position and spectral shape of BF(Mn) are also similar to those of Mn_2O_3 with the Mn^{3+} valence state in a slightly distorted octahedral symmetry.[23] Thus, BF(Mn) has the Mn^{3+} valence state. In Fig. 1, the peak position of Fe 2*p* shifts to higher energy side by about 0.1~0.2 eV. These results indicate that the Mn^{3+} electron is substituted into Fe^{2+} site, which contributes to the improvements in electrical properties in BF.

Figure 3 shows the O 1*s* XAS spectra of BF and BF(Mn), where the abscissa is the relative energy to Fermi level (E_F). The intensities of the O 1*s* XAS spectra are normalized by beam current and measurement time. From the dipole selection rule, it is understood that the O 1*s* XAS spectra of Fe oxide correspond to transitions from O 1*s* to O 2*p* hybridized with unoccupied Fe 3*d* states.[21,22,24] Therefore, the O 1*s* XAS spectra reflect the electronic structure of conduction band. The spectral shape and peak position are similar to the electronic structures of $LaFeO_3$ obtained by O 1*s* XAS and tight-binding calculation.[21] The conduction band has three structures estimated from Gaussian fitting. According to this calculation, the *a* and *b* peaks are estimated to be the minority-spin t_{2g} and e_g orbitals, respectively, because the majority-spin t_{2g} and e_g orbitals locate on the valence band side. The energy separation between *a* and *b* peaks accords with the result of Fe 2*p* XAS spectrum in Fig. 1. The *c* peak corresponds to the Bi 6*sp* state.[25,26] Such a state has been observed in unoccupied state of Bismuth layer-structured ferroelectrics.[25,26] The intensities of the minority-spin t_{2g} state (*a* peak) and Bi 6*sp* state are lower in BF(Mn), although the peak position does not change markedly. The above results indicate that the doped Mn 3*d* electron enters into minority-spin t_{2g} states of Fe 3*d* (Fe^{2+} and Fe^{3+}) and Bi 6*sp* state.

Figure 4 shows the O 1*s* SXES and XAS spectra of BF and BF(Mn), where the

abscissa is the relative energy to Fermi level (E_F). The O 1*s* SXES spectra were measured at the excitation energy of 540 eV. The O 1*s* SXES spectra, which correspond to fluorescence spectra, reflect the O 2*p* PDOS in the valence band. The energy separation between the top of the valence band and the bottom of the conduction band is the magnitude of band gap. The band gaps of BF and BF(Mn) are estimated to be 1.3 eV and 2.7 eV, respectively, by concerning the resolution in this measurement system. The small band gap of BF contributes to the low electrical resistivity of BF. The increase of band gap in BF(Mn) is closely related with the high electrical resistivity.

Figure 5(a) shows the Fe 2*p* and O 1*s* SXES spectra of BF and BF(Mn) in the valence band region. The Fe 2*p* SXES spectra were measured at the excitation energy of 740 eV. The Fe 2*p* SXES spectra, which correspond to fluorescence spectra, reflect the Fe 3*d* PDOS in the valence band. In both BF and BF(Mn), the energy position of O 2*p* state overlaps with that of Fe 3*d* state. This result indicates that the Fe 3*d* state hybridizes with O 2*p* state in the valence band. The O 2*p* valence band has three structures labeled as A, B and C. The Fe 3*d* contribution is more significant in the B and C peaks, where the O 2*p* states have a larger admixture of Fe 3*d* states. The A peak corresponds to the O 2*p* states, which have the small hybridization effect with the Fe 3*d* derived states.

As references, the Fe 3*d* PDOS curves calculated by Neaton and co-workers [27] are also shown in Fig. 5(b). They have studied theoretically the ground state structural and electronic properties of $BiFeO_3$ using the density functional theory (DFT) within the local spin density approximation (LSDA).[27] In this calculation, a large ferroelectric polarization of 90~100 $\mu C/cm^2$ is predicted, consistent with the large atomic displacements in the ferroelectric phase and with recent experimental reports.[6-9] The bandwidth of O 2*p* valence band in BF decreases with Mn substitution by about 1.0 eV, although the change of the Fe^{3+} valence state with Mn substitution is very small. They have reported that the band gap increases with increasing the electron correlation energy (U_{eff}) between Fe 3*d* states.[27] As shown in Fig. 5(a), the position of Fe 3*d* PDOS in BF(Mn) shifts to the higher energy side than that in BF. The change of bandwidth (or band gap) may contribute to the strong electron correlation with Mn substitution.

4. Conclusion

We have studied the electronic structures of BF and BF(Mn) using SXES and XAS. The BF and BF(Mn) have the mixed valence state of Fe^{2+} and Fe^{3+}. The BF(Mn) has the Mn^{3+} valence state. The valence band is mainly composed of O 2*p* state hybridized

with the majority-spin t_{2g} and e_g orbitals of Fe 3*d* state. The conduction band is composed of the minority-spin t_{2g} and e_g orbitals of Fe 3*d*. The band gaps of BF and BF(Mn) are estimated to be 1.3 eV and 2.7 eV, respectively. The Fe 3*d* PDOS of BF(Mn) shifts to the higher energy side that of BF. This behavior is similar to the result of electronic structure by DFT within LSDA method that included the effect of U_{eff}. The high electrical resistivity of BF(Mn) contributes to the increase of band gap with the increase of the electron correlation energy between Fe 3*d* states.

Acknowledgements

The Advanced Light Source is supported by the Director, Office of Science, Office of Basic Energy Sciences, of the U.S. Department of Energy under Contract No. DE-AC02-05CH11231. This work was supported by a Grant-In-Aid for Scientific Research (B) from the Ministry of Education, Culture, Sports, Science and Technology, Japan.

References

1) G. Smolenskii, V. Isupov, A. Agranovskaya and N. Kranik: Sov. Phys. Solid State **2** (1961) 2651.

2) G. Smolenskii, V. Yudin, E. Sher and Y. E. Stolypin: Sov. Phys. JETP **16** (1963) 622.

3) F. Kubel and H. Schmid: Acta Crystallogr., Sect. B **46** (1990) 698.

4) J. R. Teague, R. Gerson and W. J. James: Solid State Commun. **8** (1970) 1073.

5) D. Lebeugle, D. Colson, A. Forget, M. Viret, P. Bonville, J. F. Marucco and S. Fusil: Phys. Rev. B **76** (2007) 024116.

6) J. Wang, J. B. Neaton, H. Zheng, V. Nagarajan, S. B. Ogale, B. Liu, D. Viehland, V. Vaithyanathan, D. G. Schlom, U. V. Waghmare, N. A. Spaldin, K. M. Rabe, M. Wuttig and R. Ramesh: Science **299** (2003) 1719.

7) J. Li, J. Wang, M. Wuttig, R. Ramesh, N. Wang, B. Ruette, A. P. Pyatakov, A. K. Zvezdin and D. Viehland: Appl. Phys. Lett. **84** (2004) 5261.

8) S. K. Singh and H. Ishiwara: Jpn. J. Appl. Phys. **44** (2005) L734.

9) K. Y. Yun, D. Ricinschi, T. Kanashima, M. Noda and M. Okuyama: Jpn. J. App. Phys. **43** (2004) L647.

10) D. H. Kim, H. N. Lee, M. D. Biegalski and H. M. Christen: Appl. Phys. Lett. **92**, (2008) 012911.

11) V. R. Palkar, J. John and R. Pinto: Appl. Phys. Lett. **80** (2002) 1628.

12) Y. P. Wang, L. Zhou, M. F. Zhang, X. Y. Chen, J. M. Liu and Z. G. Liu: Appl. Phys. Lett. **84** (2004) 1731.

13) W. Sakamoto, H. Yamazaki, A. Iwata, T. Shimura and T. Yogo: Jpn. J. Appl. Phys. **45** (2006) 7315.

14) S. Yasui, H. Uchida, H. Nakaki, K. Nishida, H. Funakubo and S. Koda: Appl. Phys. Lett. **90** (2007) 22906.

15) N. Itoh, T. Shimura, W. Sakamoto and T. Yogo: Ferroelectrics **356** (2007) 19.: The details of dielectric and electrical properties have not been submitted at now.

16) A. Kotani and S. Shin: Rev. Mod. Phys. **73** (2001) 203.

17) J. C. Fuggle and J. E. Inglesfield: "*Unoccupied Electronic States*" Springer-Verlag (1991).

18) J. Nordgren and R. Nyholm: Nucl. Instrum. Methods Phys. Res. A **246** (1986) 242.

19) J. Nordgren, G. Bray, S. Cramm, R. Nyholm, J. E. Rubensson and N. Wassdahl: Rev. Sci. Instrum. **60** (1989) 1690.

20) J.-H. Guo, Y. Luo, A. Augustsson, J.-E. Rubensson, C. Såthe, H. Ågren, H. Siegbahn and J. Nordgren: Phys. Rev. Lett. **89** (2002) 137402.

21) M. Abbate, F. M. de Groot, J. C. Fuggle, A. Fujimori, O. Strebel, F. Lopez, M.

Domke, G. Kaindl, G. A. Sawatzky, M. Takano, Y. Takeda, H. Eisaki and S. Uchida: Phys. Rev. B **46** (1992) 4511.
22) H. Wadati, D. Kobayashi, H. Kumigashira, K. Okazaki, T. Mizokawa, A. Fujimori, K. Horiba, M. Oshima, N. Hamada, M. Lippmaa, M. Kawasaki and H. Koinuma: Phys. Rev. B **71** (2005) 35108.
23) J. Kawai, Y. Mizutani, T. Sugimura, M. Sai, T. Higuchi, Y. Harada, Y. Ishiwata, A. Fukushima, M. Fujisawa, M. Watanabe, K. Maeda, S. Shin and Y. Gohshi: Spectrochimica Acta. B 55 (2000) 1385.
24) T. Higuchi, T. Tsukamoto, K. Kobayashi, S. Yamaguchi, Y. Ishiwata, N. Sata, K. Hiramoto, M. Ishigame and S. Shin: Phys. Rev. B **65** (2002) 33201.
25) Y. Noguchi, M. Miyayama and T. Kudo: J. Appl. Phys. **88** (2000) 2146.
26) T. Higuchi, Y. Noguchi, T. Goto, M. Miyayama, S. Shin, K. Kaneda, T. Hattori and T. Tsukamoto: Jpn. J. Appl. Phys. **44** (2005) L1491.
27) J. B. Neaton, C. Ederer, U. V. Waghmare, N. A. Spaldin and K. M. Rabe: Phys. Rev. B **71** (2005) 014113.

Figure captions

Fig. 1 Fe 2*p* XAS spectra of BF and BF(Mn). As reference, the Fe 2*p* XAS spectrum of $LaFeO_3$ is also shown as a dashed line.

Fig. 2 Mn 2*p* XAS spectrum of BF(Mn). As reference, the Mn 2*p* XAS spectrum of $LaMnO_3$ is also shown as a dashed line.

Fig. 3 O 1*s* XAS spectra of BF and BF(Mn) presented on a relative energy compared to E_F.. Three dashed line curves are the details of conduction band that estimated from Gaussian fitting.

Fig. 4 O 1*s* SXES and XAS spectra of BF and BF(Mn) presented on a relative energy compared to E_F. The energy separation between the top of the valence band and the bottom of conduction band reflects the band gap (E_g) of BF and BF(Mn).

Fig. 5 (a) Fe 2*p* SXES spectra of BF and BF(Mn). (b) Fe 3*d* PDOS curves calculated by Neaton *et al.* (ref.27).

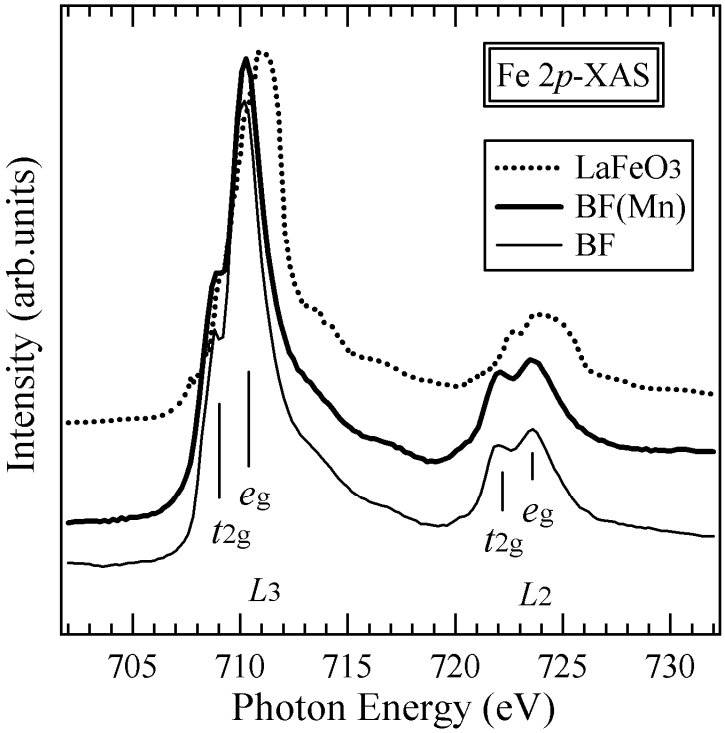

Fig. 1 T. Higuchi *et al.*

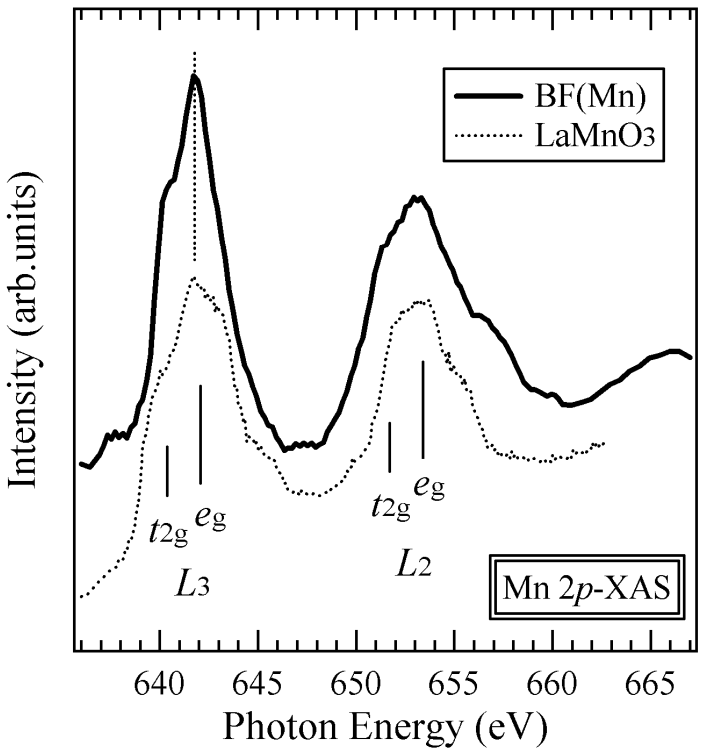

Fig. 2 T. Higuchi *et al.*

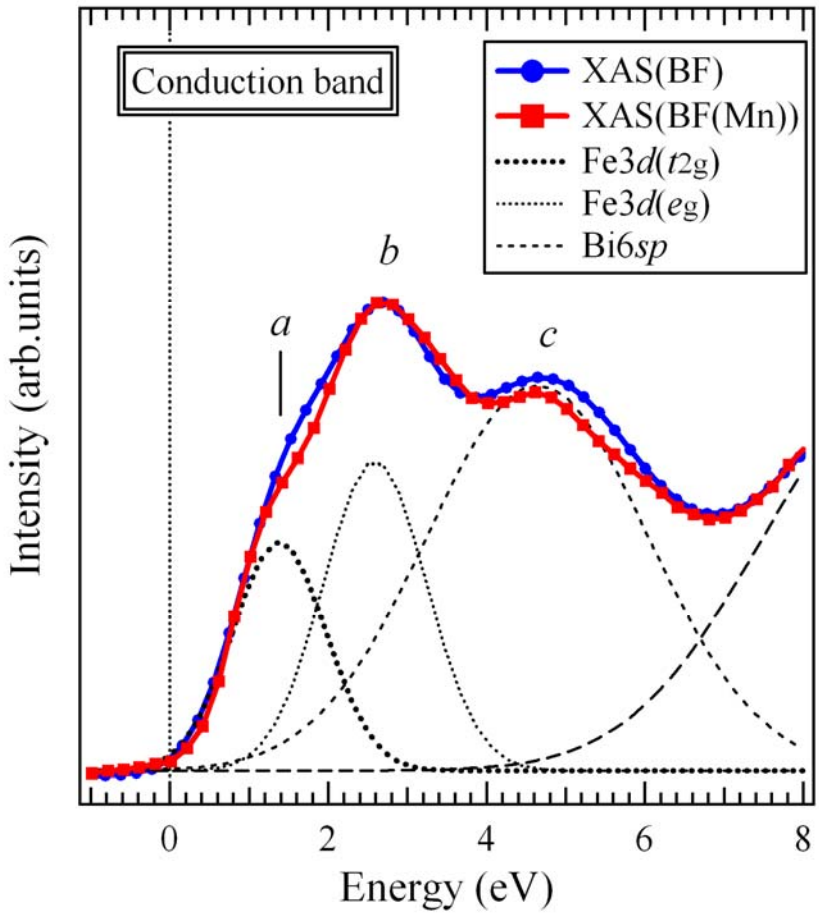

Fig. 3 T. Higuchi *et al.*

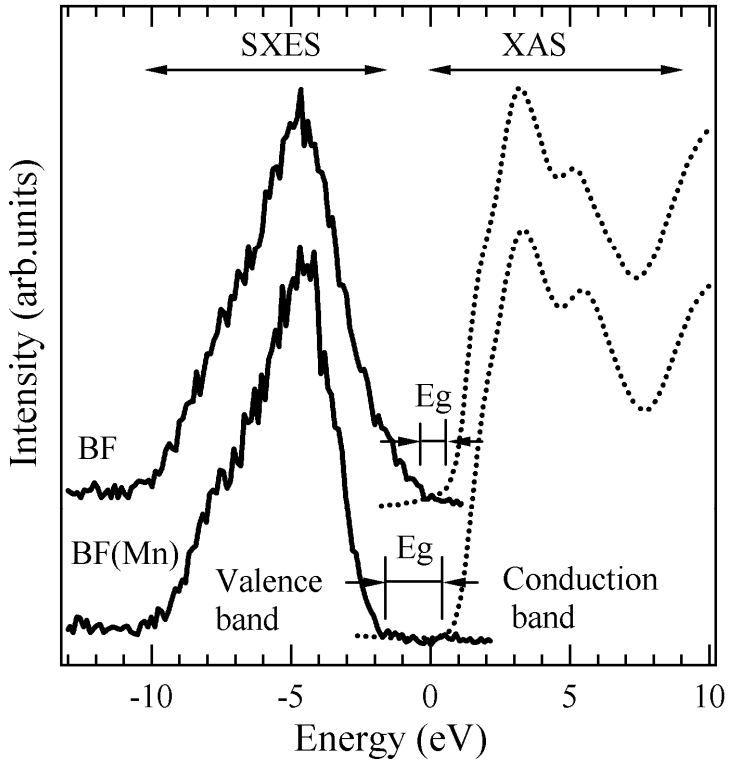

Fig. 4 T. Higuchi *et al.*

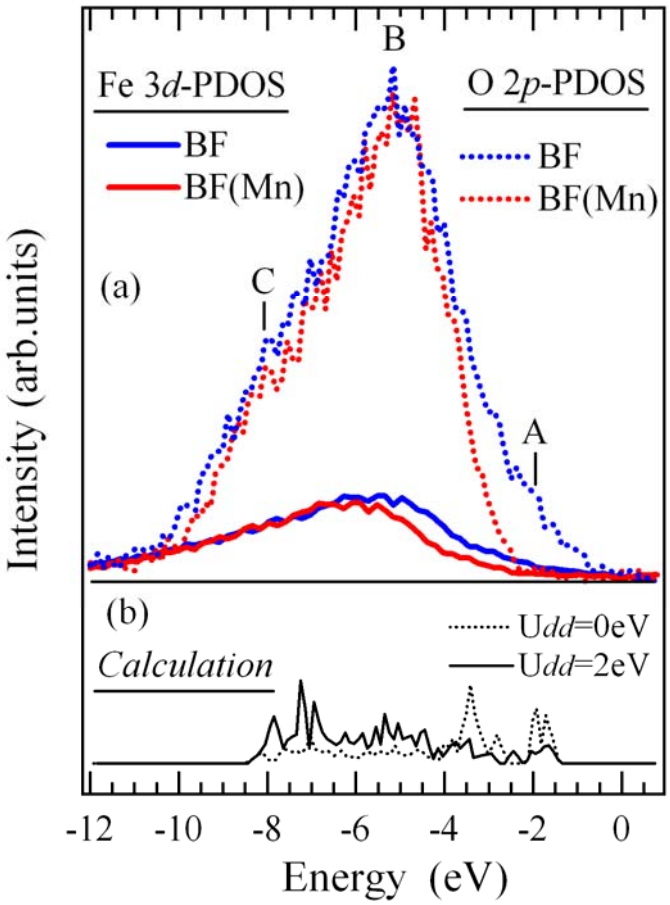

Fig. 5 T. Higuchi *et al.*